symmetry

IMPACT FACTOR 2.940

CITESCORE 4.3

Article

A Symmetry In-between the Shapes, Shells, and Clusters of Nuclei

József Cseh, Gábor Riczu and Judit Darai

Special Issue

Selected Papers from Shapes and Symmetries in Nuclei: From Experiment to Theory (SSNET'21 Conference)

Edited by

Prof. Dr. Costel Petrache and Prof. Dr. Jerzy Dudek

MDPI

https://doi.org/10.3390/sym15010115

symmetry

MDPI

Article

A Symmetry In-between the Shapes, Shells, and Clusters of Nuclei

József Cseh [1,*,†], Gábor Riczu [1,†] and Judit Darai [2,†]

[1] Institute for Nuclear Research, POB 51, 4001 Debrecen, Hungary
[2] Department of Experimental Physics, University of Debrecen, POB 400, 4002 Debrecen, Hungary
* Correspondence: cseh@atomki.hu
† These authors contributed equally to this work.

Abstract: The multiconfigurational dynamical symmetry (MUSY) connects the shell, collective, and cluster models of atomic nuclei for the case of multi-shell excitations. Therefore, it can give a unified description of various phenomena. The shape isomers are obtained from the investigation of the stability and consistency of the symmetry, and selection rules connect them to the possible cluster configurations and the related reaction channels. A simple, dynamically symmetric Hamiltonian turns out to be able to provide a unified description of the gross features of spectra of different regions of excitation energy and deformation. Some predictions of MUSY have been justified by experimental observations.

Keywords: multiconfigurational dynamical symmetry; structure models; shape isomers; clusterization; reaction channels; rotational spectra

Citation: Cseh, J.; Riczu, G.; Darai, J. A Symmetry In-between the Shapes, Shells, and Clusters of Nuclei. *Symmetry* **2023**, *15*, 115. https://doi.org/10.3390/sym15010115

Academic Editor: Charalampos Moustakidis

Received: 30 November 2022
Revised: 23 December 2022
Accepted: 27 December 2022
Published: 31 December 2022

1. Introduction

The effort of physicists in trying to understand the nuclear structure shows a close similarity to the story of the blind men who discover the elephant by touch, in the ancient Indian parable. Depending on which part their hand landed, they describe it as a thick snake, like a kind of fan, or pillar, like a tree trunk, etc.

Several features of the atomic nuclei can be described if we suppose that it is a microscopic liquid drop, which has an electric charge and undergoes collective rotation and vibration. Other characteristics make it similar to a miniature atom, with single particles orbiting in an average potential, i.e., suggest a shell model. Decay properties and nuclear reactions can be interpreted most naturally in cluster models, based on the molecular picture.

Obviously, the question, of how the fundamental structure models are related to each other is essential. (We would like to know, what the whole elephant looks like.) A real breakthrough came in 1958. It turned out that the SU(3) symmetry connects the spherical shell model, the quadrupole collective model [1,2] and the cluster model to each other [3,4]. Applying the present-day terminology, we can say that the common intersection of the three basic models is provided by the

$$U(3) \supset SU(3) \supset SO(3) \tag{1}$$

dynamical symmetry. This beautiful relationship was established for a single shell problem.

To find the connection for the general problem, including major shell excitations, much effort was concentrated on various theoretical frameworks in the following decades, and several aspects have been clarified.

Here, we present a symmetry-based relation between the three fundamental models for the multi-major-shell problem. It is a simple generalization of the historical dynamical symmetry (1):

$$U_e(3) \otimes U_s(3) \supset U(3) \supset SU(3) \supset SO(3). \tag{2}$$

(The exact meaning of the first two groups is discussed below.) This dynamical symmetry, called multiconfigurational dynamical symmetry (MUSY), provides us with the common intersection of the shell, collective, and cluster models for the multi-shell problem. It looks quite natural, almost straightforward. Nevertheless, it took a long time until the fully algebraic shell, collective, and cluster models were developed for the many major shell problem, and their connection was revealed. Here the fully algebraic indicative refers to a description, in which not only the basis states but also the physical operators carry some group symmetries, like in the Elliott model [1,2]. In fact, MUSY is a composite symmetry in the sense that in addition to the dynamical symmetry (2) of each configuration, there is a further symmetry that connects the different configurations to each other. This latter one acts in the pseudo space of the particle indices. Further discussion is presented in the next section.

Since MUSY is bridging the shell and collective models, it allows us to determine the stable quadrupole shapes of nuclei from the symmetry of the shell model. So it offers a possibility, which is an alternative to the usual energy-surface calculations. In particular, the shape isomers are obtained from the investigation of the Stability and Consistency of the connecting U(3) Symmetry (called the SCS method). Since the U(3) symmetry uniquely defines the quadrupole deformation, we can also say that the stability and consistency of the deformation are investigated.

MUSY connects the shell model not only to the collective but also to the cluster model; therefore, one can apply a U(3) selection rule for the determination of the allowed cluster configurations. The cluster configurations have a direct connection to the reaction channels; thus, one can determine easily in which channels the shape isomers can be populated, or decay.

One of the nice features of the dynamical symmetries is that they offer an analytical solution for the eigenvalue problem, and so does the MUSY as well. Therefore, it is easy to apply for the description of a large amount of experimental data. It turns out, that it can give a unified description of spectra of different configurations in different energy regions and in a wide range of deformation.

The nuclear deformation is a result of spontaneous symmetry breaking. In particular, the rotational SO(3) symmetry is broken in the eigenvalue problem of the intrinsic Hamiltonian. The simplest manifestation of this phenomenon shows how the quadrupole deformation appears in the spherical shell model (Elliott model and its extensions) [5]. In the cluster model, the same scenario results in more exotic molecular configurations. Since MUSY connects the shell and cluster models (of different configurations) to each other, it sheds some new light on the long-standing problem of cluster-shell competition or duality as well.

The structure of this paper is as follows. In Section 2, first, we recall the basic features of the 1958 connection, and afterward, we introduce the MUSY and review its main characteristics very briefly. In Section 3, we present some applications of MUSY. They give unified descriptions of different phenomena, which are usually treated in different manners. Finally, in Section 4, a brief summary is given, and some conclusions are drawn.

2. Connecting Symmetry

2.1. Single-Shell Problem

In 1958, Elliott showed that the quadrupole deformation and the collective rotation could be obtained from a spherical shell model by selecting well-defined SU(3) symmetries [1,2]. The average potential of the Elliott model is that of the harmonic oscillator, and the residual nucleon–nucleon interaction is quadrupole type: $Q^a \cdot Q^a$. Here Q^a is the algebraic quadrupole operator, which acts only within a major shell, and is obtained as a summation of the nucleon quadrupole operators:

$$Q^a_{2q} = \sqrt{\frac{4\pi}{5}} \sum_{n=1}^{A} \left(\frac{x_n^2}{b^2} Y_{2q}(\hat{x}_n)\right) + b^2 p_n^2 Y_{2q}(\hat{p}_n),$$

where b stands for the oscillator parameter $b = \sqrt{\hbar/2\omega}$. This operator has non-vanishing matrix elements only between states of the same major shell. (The physical quadrupole operator

$$Q^c_{2q} = \sqrt{\frac{16\pi}{5}} \sum_{n=1}^{A} \frac{x_n^2}{b^2} Y_{2q}(\hat{x}_n)$$

on the other hand, connects also states with ± 2 oscillator quanta difference. Its matrix elements within a major shell coincide with those of Q^a.) The scalar product $Q^a \cdot Q^a$ can be expressed as the linear combination of the (quadratic) invariant operators of the SU(3) ($C^{(2)}_{SU3}$) and SO(3) ($C^{(2)}_{SO3} = L^2$) algebras: $Q^a \cdot Q^a = 6C^{(2)}_{SU3} - 3L^2$. Since the harmonic oscillator Hamiltonian H_{HO} is the linear invariant of the U(3) algebra, the Hamiltonian of the Elliott model can be written as a linear combination of the invariant operators of the algebra chain (1):

$$H = H_{HO} - \frac{1}{2}\chi Q^a \cdot Q^a = C^{(1)}_{U3} - 3\chi C^{(2)}_{SU3} + \frac{3}{2}\chi C^{(2)}_{SO3}. \quad (3)$$

This latter algebraic form guarantees that the representation labels of the algebras in the chain (1) provide a complete classification scheme on the basis $(U(3) : [n_1, n_2, n_3], SU(3) : (\lambda, \mu), K, SO(3) : L$, where K distinguishes between different SO(3) representation within an SU(3) one). Furthermore, the energy eigenvalue problem has an analytical solution:

$$E = \hbar\omega n - 3\chi(\lambda^2 + \mu^2 + \lambda\mu + 3\lambda + 3\mu) + \frac{3}{2}\chi L(L+1).$$

Elliott showed that the quadrupole shape of the nucleus is determined by the (λ, μ) SU(3) quantum numbers. For example, (0, 0) is spherical $(\lambda, 0)$ is prolate with cylindrical symmetry, $(0, \mu)$ is oblate, and in general (λ, μ) has a triaxial shape. The quantitative relation by which the SU(3) symmetry determines the quadrupole deformation is [6,7]:

$$\beta^2 = \frac{16\pi}{5N_0^2}(\lambda^2 + \mu^2 + \lambda\mu),\ \gamma = arctan(\frac{\sqrt{3}\mu}{2\lambda + \mu}). \quad (4)$$

Here, N_0 is the number of oscillator quanta, including the zero point contribution: $N_0 = n + (A-1)\frac{3}{2}$, n is the sum of the U(3) quantum numbers: $n = n_1 + n_2 + n_3$, and A is the mass number of the nucleus.

Let us pay attention to the breaking of symmetries in Equation (3). Not only because it is important in the Elliott model, but also due to the fact that this model is the prototype of the algebraic structure models; therefore, the same scenario is present in many other approaches, too. As it is well known, the three-dimensional harmonic oscillator has an exact U(3) symmetry. Therefore, the Hamiltonian H_{HO} provides a spectrum of equidistant energies and complete degeneracy within a major shell. The rest of H, however, breaks the U(3) symmetry; thus, the degeneracy is lifted. Nevertheless, this kind of special breaking (when the interactions are written in terms of the invariant operators of a single algebra chain) does not mix the representations, and their labels remain good quantum numbers; furthermore, the analytical solution is still available. It is called dynamical symmetry breaking. It is well known for a long time, and many other structure models share this feature. Usually, the complete algebra chain is said to define a dynamical symmetry [8].

There is, however, another symmetry breaking in the Elliott model as well, which is not very well known. In particular, the rotational SO(3) symmetry breaks spontaneously, and this spontaneous breaking results in a deformed shape. The fact that nuclear deformation is a result of spontaneous symmetry breaking has been accepted for a long time, but it was discussed either in the mean-field model, or in the interacting boson model, but not in the Elliott model [8–11]. This is somewhat surprising, considering that the first explanation of the deformation and collective rotation from the spherical shell model viewpoint was given by the Elliott model. In fact, it offers a very simple and transparent illustration of the

spontaneous breaking [5]. It is obvious from Equation (3), that the Hamiltonian can be split up into an intrinsic and a collective part:

$$H = H_{int} + H_{coll}, \;\; H_{int} = C^{(1)}_{U3} - 3\chi C^{(2)}_{SU3}, \;\; H_{coll} = \frac{3}{2}\chi C^{(2)}_{SO3}.$$

The first term determines the band heads, while the second splits up the bands. The first one contains the fast, and the second the slow degrees of freedom. Both of them are rotationally invariant; however, in the eigenvalue problem of the intrinsic Hamiltonian, one obtains a deformed ground state for most of the nuclei. This phenomenon, namely the non-symmetric ground state of a symmetric Hamiltonian, is known as spontaneous breaking.

So, the Elliott model shows a dual breaking of symmetries: the U(3) and SU(3) symmetries are dynamically broken by the interactions of the model, while the rotational symmetry is spontaneously broken in the eigenvalue problem of the intrinsic Hamiltonian. This kind of duality of symmetry breaking is also very common in nuclear structure models [12].

Still, in 1958 Wildermuth and Kanellopoulos established the connection between the shell model and cluster model wave functions [3], by rewriting the model Hamiltonians into each other in the harmonic oscillator approximation

$$H^{cl}_{HO} = H^{sm}_{HO}.$$

This relation of the Hamiltonians establishes, of course, a close connection also between the eigenstates. In particular, any cluster state can be expanded in terms of shell states of the same energy. This essential relation between the operators and states is valid not only for the HO interactions but also for more general ones [13]. It plays a fundamental role in relating the basis states of different models or different configurations to each other. More discussion along this line comes later.

Bayman and Bohr could reinterpret the cluster–shell connection in terms of SU(3) symmetry [4]. Therefore, the interrelation of the basic models was found in 1958 in terms of the SU(3) symmetry. In particular, the quadrupole collective states, as well as the cluster bands, could be picked up from the see of the shell model states by their specific SU(3) symmetry.

2.2. Multi-Shell Problem

2.2.1. Structure Models

The SU(3) shell model, as invented by Elliott [1,2], is a single-shell model: one considers an inert core, and the valence nucleons occupy a single major shell. The model turned out to be very successful in the description of the *p*, and *sd* shell nuclei. Nevertheless, it can describe the electromagnetic transitions only with an effective charge, which is a phenomenological parameter. To reproduce the experimental data with real nucleon charges, one has to take into account major shell excitations. Several other physical phenomena require this extension along the vertical energy scale, too. A successful algebraic shell model of the many major shell problem was invented by Rosensteel and Rowe [14], known as the symplectic shell model. In this model, the U(3) symmetry of the Elliott model is embedded in the Sp(6,R) real symplectic group:

$$Sp(6,R) \supset U(3) \supset SU(3) \supset SO(3).$$

(Note, that some authors denote the same group by Sp(3,R).) The symplectic group has several interesting features.

(i) It preserves the equilibrium shape of the nucleus under transformations, such as rotations, orientations in space and vibrations [15,16].
(ii) It contains the linear canonical transformations of nucleon coordinates and momenta, that preserve Heisenberg's commutation relations.

(iii) Its generators include the total kinetic energy, the monopole and quadrupole moment, the angular momentum, and the many-particle HO Hamiltonian.

The quadrupole operator is not the algebraic one, as in the Elliott model, but rather the physical one. Therefore, it connects the major shells with ± 2 oscillator quanta, i.e., the neighboring shells with the same parity. An irreducible representation (irrep) of it spans the full positive (or negative) parity spectrum of the HO.

Sp(6,R) contains several subgroups, but the actual calculations are carried out within the symplectic shell model by applying the U(3) subgroup chain, mentioned here. Then a symplectic representation is built on a U(3) representation $[n_1^s, n_2^s, n_3^s]$, and the raising or lowering operators also have U(3) tensorial character ($[n_1^e, n_2^e, n_3^e]$); therefore, the representation of the U(3) dynamical symmetry (1) are embedded in the product representation of $[n_1^e, n_2^e, n_3^e] \otimes [n_1^s, n_2^s, n_3^s]$. Please, note that this is exactly the structure of the set of the basis of the MUSY (2).

The Sp(6,R) symplectic model is a multi-shell extension of the SU(3) shell model, and at the same time, it is a microscopic version of the collective model. In its original version, it is a traditional shell model in the sense that some of the nucleons form a closed core. Recently it was generalized to a no-core model [17], in which all the nucleon degrees of freedom are taken into account. Therefore, it represents a real ab initio method, when realistic nucleon-nucleon forces are applied.

The algebraic no-core approach can use not only the symplectic basis but also the SU(3) basis when it is called the symmetry-adapted no-core shell model (SA-NCSM) [18,19]. This is also a many major shell (no-core) extension of the Elliott model, of course. When truncating its model space to the spin–isospin zero (i.e. Wigner-scalar) sector, one arrives at the semimicroscopic algebraic quartet model (SAQM) [20]. It is usually equipped with simple, dynamically symmetric interactions, and it is one of the building blocks of MUSY, as we discuss in further detail below.

The symplectic model has a simplified version, called the contracted symplectic model [21,22]. From the mathematical viewpoint, the simplification takes place due to the group deformation mechanism: in the large $n(= n_1^s + n_2^s + n_3^s)$ limit, the Sp(6,R) group approximates the $\mathrm{U}_e(6) \otimes \mathrm{U}_s(3)$ direct product group. This is a compact group, which has finite representations, and its basis states are orthogonal (while Sp(6,R) is noncompact, and the orthogonality is not valid either). The group deformation takes place by substituting the operators creating or annihilating the 2 (or 0) oscillator quanta of the major shell excitations, by a simple boson operator. Therefore, $\mathrm{U}_e(6)$ has exactly the same realization, as that of the interacting boson model (IBM); nevertheless, their physical contents are different: in the contracted symplectic model, the bosons correspond to inter shell excitations, while in IBM intra shell excitations. The bosonization also involves that the antisymmetrization of the wave function is only approximate in the contracted model (while it is complete in the symplectic model). The contracted symplectic model contains the dynamical symmetry group (2) as a subgroup chain:

$$U_e(6) \otimes U_s(3) \supset U_e(3) \otimes U_s(3) \supset U(3) \supset SU(3) \supset SO(3).$$

As for the clusterization is concerned, the relevant approach for revealing the connection to other structure models needs to be fully algebraic, and at least (semi)microscopic, i.e., the model space has to be constructed microscopically. The semimicroscopic algebraic cluster model [23,24] has these essential features. In this model, the internal structure of the clusters is described by Elliott's SU(3) shell model, while the relative motion is treated in terms of the vibron model [25,26]. Its model space is constructed to be free from the Pauli-forbidden states [23,24]. For a binary clusterization, its algebraic structure and basis are characterized by the group chain:

$$U_{C_1}(3) \otimes U_{C_2}(3) \otimes U_R(4) \supset U_C(3) \otimes U_R(3) \supset U(3) \supset SU(3) \supset SO(3).$$

where C_1 and C_2 stand for individual clusters, C is for their coupled structure, and R indicates relative motion. Please note the presence of group chain (2).

In the symplectic, contracted symplectic, and cluster models, we were dealing only with the space degrees of freedom and did not discuss the spin–isospin sector. It can be described in each case by Wigner's supermultiplet theory of $U^{ST}(4) \supset U^{S}(2) \otimes U^{T}(2)$, just like in the Elliott model. The antisymmetric requirement of the total wave function puts a constraint on the relation between the irreducible representation of $U^{ST}(4)$ and $U(3)$, which are taken into account in each major shell separately, and then they are combined [27].

2.2.2. Transformations and Symmetries

The group chain (2) and its representation labels provide us with the possibility of classifying the basis states of different configurations according to the same symmetries. This is a major step towards the unified description of different spectra. However, the story of the multiconfigurational dynamical symmetry is not complete with this recognition. We also need the transformations, which connect the different configurations, and their dynamical symmetries to each other.

With respect to the connecting symmetries, one can follow different logical paths. First, MUSY was realized as a symmetry connecting different (binary) cluster configurations [28], for example, ^{24}Mg+^{4}He and ^{16}O+^{12}C in ^{28}Si. Then the reasoning was based on the connection of the wave functions and energy eigenvalues: when the wave functions of the (seemingly) different clusterization are identical due to the antisymmetrization, one can *require* that their energies should be the same. For the simple case of the two binary cluster configurations, the underlying transformations and symmetries were found later in terms of the Talmi–Moshinsky transformation [29]. The finding that the shell model (or the quartet model) fits the same scheme of MUSY came later [20,30,31]. Finally in [27] the general mathematical formalism was given that includes any number of shell and cluster configurations and guides us in finding the interactions which are invariant with respect to the transformations between them.

The symmetry that connects the different configurations to each other is based on a classification scheme, which is different from that of the group chain (2). In particular, so far we have been following a structure, which is guided by the shell scheme: the symmetries (permutational, spin–isospin, and spatial symmetries) of the nucleons were treated in each major shell separately, and then combined together. The connecting symmetry follows a different path, called a particle scheme. It is based on the study of Kramer and Moshinsky [32] of the n-particle system in a harmonic oscillator potential. This system has a U(3n) symmetry group, and its subgroups: U(3) in the real space and U(n) in the particle index space U(3n) $\supset$ U(3) $\otimes$ U(n). The generators of these groups are the number-conserving bilinear products of the oscillator quantum creation and annihilation operators. In particular, there are 3n $\times$ 3n of them for U(3n), 3 $\times$ 3 for U(3), and nxn for U(n). The generators of the subgroups are obtained from those of U(3n) by contraction, i.e., summing up according to the particle indices for U(3), and according to the space indices for U(n) [27,32]. The transformations from one configuration to the other correspond to rearrangements in the particle index pseudo space, i.e., elements of the U(n) group. (In the spin–isospin space, the symmetry group is U(4n), which is contracted in a similar way.) When we apply interactions (or operators in general), which are expressed in terms of the contracted generators of U(3), they are invariant with respect to all the transformations between the different configurations.

3. Application

3.1. Shape Isomers

In the low-energy region of light nuclei, U(3) turns out to be a good approximate symmetry, as found by Elliott [1,2]. Due to the symmetry-breaking interactions, like spin-orbit, and pairing, however, it breaks down with increasing energy, and the whole spectrum can not be characterized by U(3). Surprisingly enough, however, a generalized version of it,

called quasi-dynamical U(3) symmetry, is a good approximation even in the presence of large symmetry-breaking interactions, like spin-orbit and pairing [33].

The quasi-dynamical symmetry (QDS) is probably the most general symmetry concept of quantum mechanics. It is a symmetry of the eigenvalue equation when neither the operator nor its eigenvectors are symmetric, i.e., the operator is not a scalar, and the eigenvectors do not transform according to an irreducible representation. Yet symmetry is present and has important consequences. The mathematical reason for this unexpected symmetry is the embedded representation. It can be obtained as follows: take the operators, which generate the U(3) group, and calculate their matrix elements between energy eigenstates. When the eigenstates are U(3) basis states, we end up with the matrix representation of the group. If the eigenstates are linear combinations of U(3) basis sates belonging to inequivalent U(3) representations, then the matrices are different and do not give, in general, a representation. It may happen, however, that for some special linear combinations, the matrices coincide with those of a representation either exactly, or approximately. Then one speaks about (exact or approximate) embedded representation, which indicates (exact or approximate) quasi-dynamical (or effective) symmetry [34,35]. (An embedded representation involves only a part of the total Hilbert space.) The appearance of the QDS seems like a spontaneous building up of symmetry.

The quasi-dynamical generalization allows us to investigate the stability and self-consistency of the SU(3) symmetry, called the SCS method. Due to Eqs. (4) it means the investigation of the stability and self-consistency of the quadrupole shape [36]. The effective SU(3) quantum numbers can be determined from the occupation of the asymptotic Nilsson orbitals [37], therefore, the following scenario is applied.

(i) Determine the Nilsson-orbitals as a function of the quadrupole deformation parameters.
(ii) Obtain the many-particle state by filling in the Nilsson orbitals according to the energy minimum and Pauli-exclusion principle.
(iii) Expand the single-particle orbitals in terms of the asymptotic Nilsson-states [38].
(iv) Determine the effective SU(3) quantum numbers from the linear combinations of (iii) and from the relations of the large deformation.
(v) The effective quantum numbers can be translated to the parameters of the quadrupole deformation.

The result is a stair-like function, as shown schematically in the lower case of Figure 1. The horizontal platos correspond to the shape isomers, indicating the stability and the self-consistency of the SU(3) symmetry (or deformation parameter). For comparison, the upper case illustrates the (schematic) result of the usual energy-surface calculation.

The shape isomers of the ^{28}Si and ^{36}Ar nuclei obtained from the SCS method are shown in Figures 2 and 3, respectively, and they are compared with the results of other models in Table 1. As is seen in the figures, the effective U(3) quantum numbers have some small uncertainty for the shape isomers. Here we indicated the most typical ones.

Table 1. Shape isomers of the ^{28}Si and ^{36}Ar nuclei from different model calculations. The results of the Nilsson energy-surface calculations are from the work [39], the alpha-cluster model calculations (for one, two, and three-dimensional configurations) are presented in [40–42], while the column "SCS-method" refers to the shape self-consistency model. The abbreviations are as follows: GS: ground state, α-ch: alpha chain, Tri: triaxial, Pro: prolate, Obl: oblate. The notations of the alpha-cluster configurations are: 2D means 2-dimensional configuration; in these cases the parentheses contain the ratio of ($\omega_y : \omega_x$), $\hbar\omega$ indicates the number of excitation quanta, (ϵ,γ) are the parameters of the quadrupole deformation (γ is given in degrees), and a:b:c stands for the ratio of the major axes of the ellipsoid.

Nucl.	$\hbar\omega$	**Energy Surface**		**Alpha-Cluster**			**SCS-Method**	
		ω_x:ω_y:ω_z (ϵ,γ)	**U(3)**	**Shape**	**U(3)**	$U(3)_{eff}$	(ϵ,γ)	**a:b:c**
^{28}Si						[14,13,9]	(0.19,49)	1.2:1.2:1
	0	3:3:2 (0.45,0)	[20,8,8]	Pro (GS)	[20,8,8]	[19,9,8]	(0.44,5)	1.5:1.0:1
		2:1:1 (0.49,60)	[16,16,4]	Obl	[16,16,4]	[16,15,5]	(0.44,55)	1.6:1.5:1
	4			Tri	[28,8,4]	[27,7,5]	(0.84,5)	2.2:1.1:1
	8			2D (3:2)	[24,20,0]	[24,20,0]	(0.84,51)	2.7:2.4:1
				2D (3:2)	[28,16,0]	[26,11,7]	[0.7,12)	1.9:1.2:1
		(1.35.60)	[32,8,4]					
	12			2D (3:1)	[36,12,0]	[35,8,5]	(1.0,5)	2.6:1.6:1
		(1.0,0)	[40,4,4]	Pro (4:1)	[40,4,4]	[40,4,4]	(1.3,0)	3:1:1
	16	6:3:1 (1.32,35)	[44,8,0]					
	28					[59,3,1]	(1.7,2)	4.9:1.1:1
	48			α-ch	[84,0,0]	[84,0,0]	(2.1,0)	7:1:1
^{36}Ar	0	3:2:2 (0.29,60)	[20,20,12]	GS	[20,20,12]	[20,19,13] [20,18,15]	(0.2,52) (0.1,37)	1.2:1.2:1 1.2:1.1:1
	4					[26,22,8]	(0.5,48)	1.7:1.5:1
				Tri	[32,16,8]	[30,15,11]	(0.5,12)	1.7:1.1:1
	8					[30,25,5]	(0.6,49)	2.1:1.9:1
		(0.74,7)	[40,12,8]			[39,12,9]	(0.8,5)	2.1:1.1:1
	12			Tri	[48,8,8]	[47,9,8]	(1.0,1)	2.5:1.0:1
	16			2D (4:1)	[40,28,0]			
		(1.45,55)	[48,12,8]					
	20					[40,32,0]	(0.9,49)	3.2:2.8:1
				2D (2:1)	[52,20,0]			
		(1.33,47)	[56,12,4]					
	24					[63,7,5]	(1.4,2)	3.5:1.1:1
	28			2D (3:1)	[64,16,0]			
	92			α-ch	[144,0,0]	[144,0,0]	(2.3,0)	9:1:1

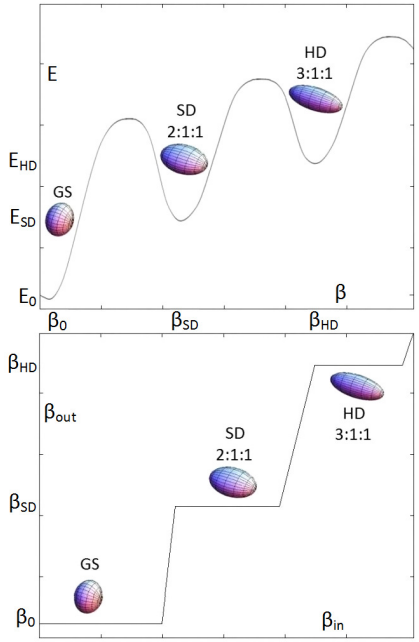

Figure 1. Schematic illustration of the appearance of the SD and HD shapes in the energy-minimum and in the deformation stability and self-consistency calculation.

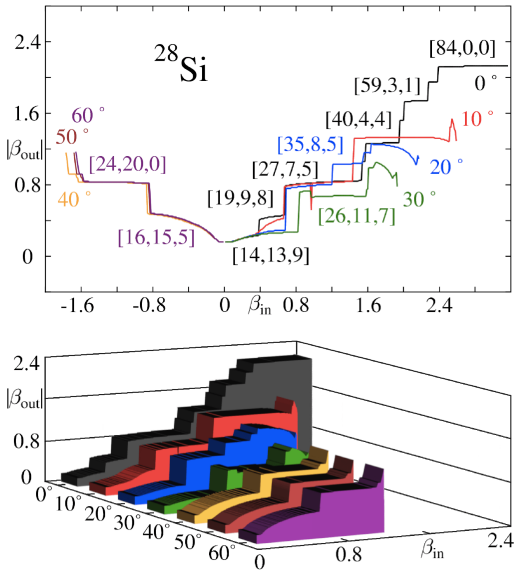

Figure 2. Shape isomers of the ^{28}Si nucleus from the SCS method using effective U(3) quantum numbers. In the upper part, the horizontal axis shows the β_{in} input parameter; the vertical axis indicates the value of β_{out}. The γ parameter is given in degrees, and steps in 10. The lower part shows the same result in three dimensions.

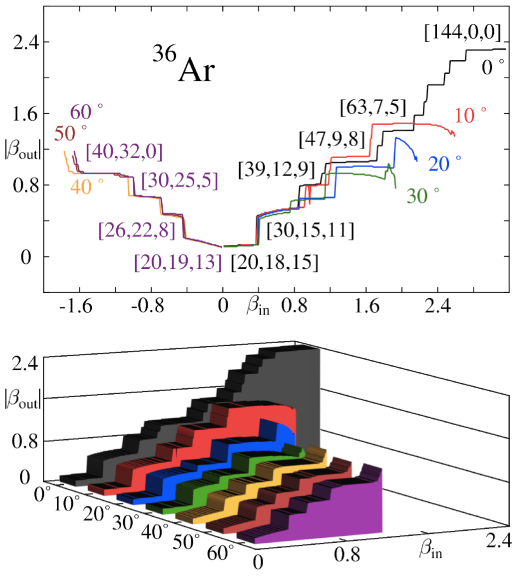

Figure 3. The same as Figure 2, for ^{36}Ar.

3.2. Clusterization and Reaction Channels

Since the shape isomers are characterized by their spatial U(3) and spin–isospin $U^{ST}(4)$ symmetries, their possible binary clusterization can be easily determined by selection rules. Furthermore, the cluster configurations are related to reaction channels (in fact, they are defined by the reaction channels); thus, we obtain information on the possible binary reaction channels, which can populate the shape isomers, or in which they can decay.

For a binary cluster configuration, the U(3) selection rule reads

$$[n_1, n_2, n_3] = [n_1^{(1)}, n_2^{(1)}, n_3^{(1)}] \otimes [n_1^{(2)}, n_2^{(2)}, n_3^{(2)}] \otimes [n^{(R)}, 0, 0]$$

where $[n_1, n_2, n_3]$ is the set of U(3) quantum numbers of the parent nucleus, the superscript (i) stands for the i'th cluster, and (R) indicates relative motion. Characterizing the nuclei (clusters) by their U(3) symmetry means that they are supposed to be in their ground intrinsic states, but collective excitations (belonging to the same irreducible representation) are incorporated. The clusters have deformation (prolate, oblate, triaxial) like real nuclei, and their relative orientation is not restricted in any way. The U(3) selection rule, which deals with the spatial symmetry of the states, is always accompanied by a similar $U^{ST}(4)$ selection rule

$$[f_1, f_2, f_3, f_4] = [f_1^{(1)}, f_2^{(1)}, f_3^{(1)}, f_4^{(1)}] \otimes [f_1^{(2)}, f_2^{(2)}, f_3^{(2)}, f_4^{(2)}]$$

for the spin–isospin degrees of freedom.

When a given cluster configuration is forbidden, we can characterize its forbiddenness quantitatively in the following way. The distance between the U(3) representations of the parent nucleus and a cluster configuration is defined as

$$min(\sqrt{(\Delta n_1)^2 + (\Delta n_2)^2 + (\Delta n_3)^2}),$$

where $\Delta n_i = |n_i - n_{i,k}^c|$. Here n_i refers to the U(3) representation of the parent nucleus, while $n_{i,k}^c$ stands for the U(3) representation of channel c, obtained from the multiplication, with the k index distinguishing the different product representations. Based on this quantity we determine, for reasons of convenience, the reciprocal forbiddenness, S in such a way, that $0 \leq S \leq 1$:

$$S = \frac{1}{1 + min(\sqrt{(\Delta n_1)^2 + (\Delta n_2)^2 + (\Delta n_3)^2})}.$$

Then $S \approx 0$, and $S \approx 1$ correspond to completely forbidden and completely allowed cluster configurations, respectively.

The reciproc forbiddenness of different clusterization of the shape isomers of the ^{28}Si and ^{36}Ar nuclei are shown in Figures 4 and 5, respectively. In these figures, we characterize the shape isomers by the U(3) symmetries, which correspond to the simplest shell configuration, and coincide also with those of the alpha-cluster calculations (when they are found).

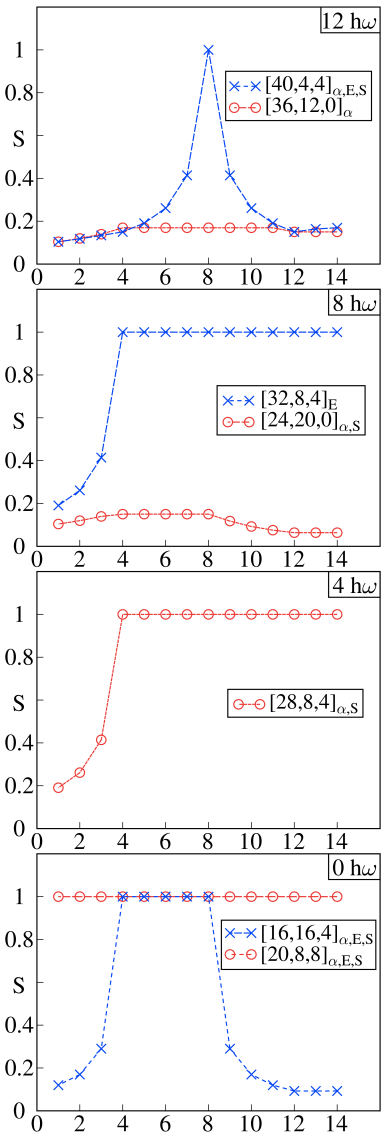

Figure 4. Reciprocal forbiddenness as a function of the mass number of the lighter cluster for the shape isomers in ^{28}Si. The lines are just to guide the eye.

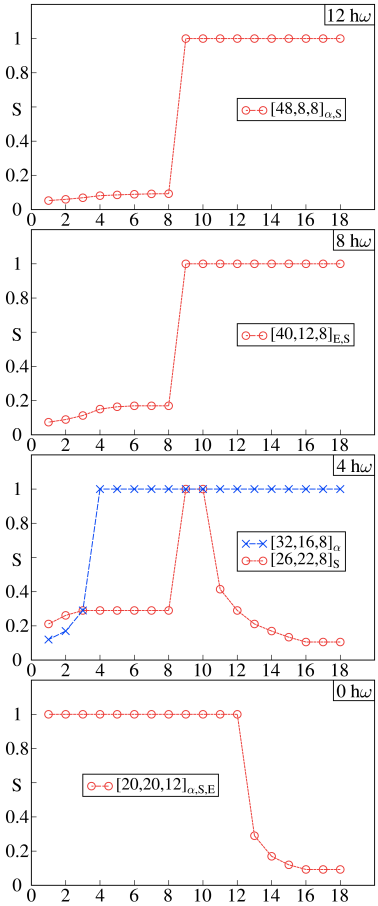

Figure 5. The same as Figure 4, for ^{36}Ar. The indices indicate in which model appears the nuclear shape corresponding to a given representation. S: SCS-method, E: Energy surface, α: α cluster.

3.3. Spectra

We apply a simple Hamiltonian, expressed in terms of the invariant operators of the U(3)⊃SU(3)⊃SO(3) algebra chain.

$$\hat{H} = (\hbar\omega)\hat{n} + a\hat{C}^{(2)}_{SU3} + b\hat{C}^{(3)}_{SU3} + d\frac{1}{2\theta}\hat{L}^2, \tag{5}$$

The first term is the harmonic oscillator Hamiltonian (linear invariant of the U(3)), with a strength obtained from the systematics [43] $\hbar\omega = 45A^{-\frac{1}{3}} - 25A^{-\frac{2}{3}}$ MeV. Its value is 12.1080 MeV for ^{28}Si and 11.3354 MeV for ^{36}Ar. The last one is the rotational term with a parameter to fit, (θ is the moment of inertia calculated classically for the rigid shape determined by the U(3) quantum numbers (for a rotor with axial symmetry) [20].) The remaining parts were written in terms of the second ($\hat{C}^{(2)}_{SU3}$) and third order ($\hat{C}^{(3)}_{SU3}$) invariant of the SU(3). The former one accounts for the quadrupole–quadrupole interaction, and the latter one distinguishes between the prolate and oblate shapes. This Hamiltonian turned out to be successful in describing the low-energy quartet spectra of light nuclei [20,31], and predicting from them the high-lying cluster spectra [31,44], as it is shown in Figures 6–9, respectively. The parameters are given in Table 2. More detailed discussions of the results are given in the concluding section.

The intraband $B(E2)$ value is given by [20]:

$$B(E2, I_i \to I_f) = \frac{2I_f + 1}{2I_i + 1}\alpha^2 |\langle (\lambda,\mu)KI_i, (11)2||(\lambda,\mu)KI_f\rangle|^2 C^{(2)}(\lambda,\mu), \tag{6}$$

where $\langle (\lambda,\mu)KI_i, (11)2||(\lambda,\mu)KI_f\rangle$ is the SU(3) $\supset$ SO(3) Wigner coefficient [45], and α is a parameter fitted to the experimental value of the $2_1^+ \rightarrow 0_1^+$ transition. The interband transition rate is zero.

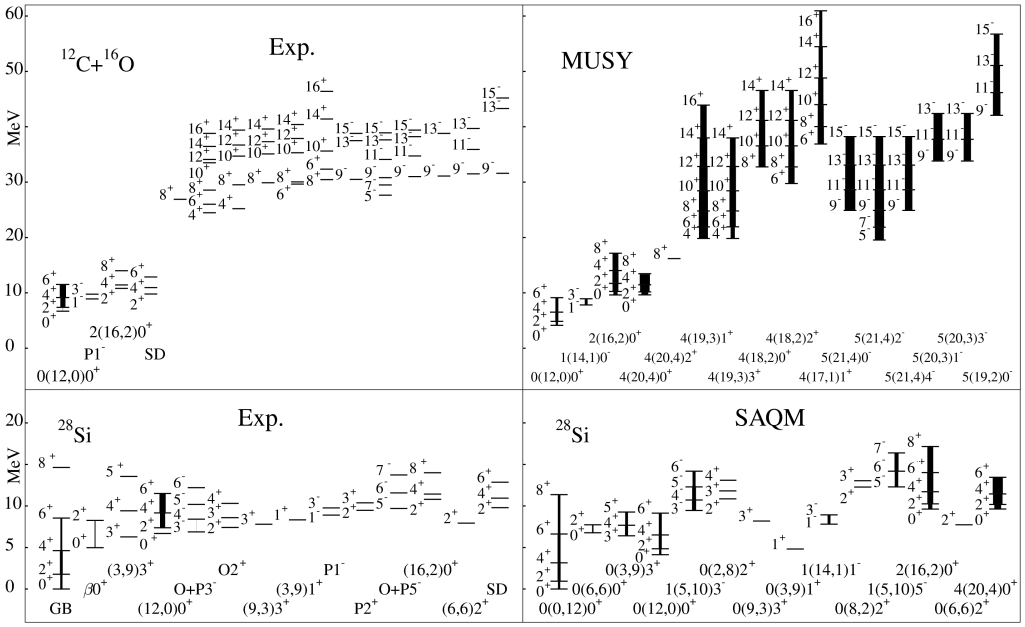

Figure 6. The spectrum of the MUSY in comparison with the experimental data of the ^{28}Si nucleus. The experimental bands are labeled by the available quantum numbers. The parameters have been fitted to the low-energy part (lower panel), and the cluster spectrum (upper panel) is obtained as a pure prediction, due to the unified multiplet structure and identical physical operators.

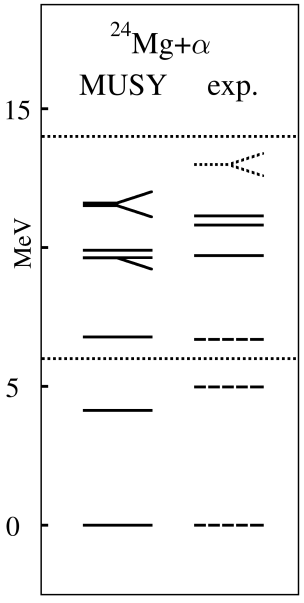

Figure 7. Comparison of the ^{24}Mg+^{4}He 0^+ spectra from the theoretical prediction (of Figure 6) and the experimental observation. The energy window of the [44] experiment is indicated by the dotted lines in both panels. In the experimental part the solid lines show the observed resonances of [44], the dotted Y-shaped lines are the states from the ^{24}Mg+^{4}He measurements which are not resolved in [44]. The dashed lines correspond to known low-lying 0^+ states which were not measured at 0° in [44] experiment.

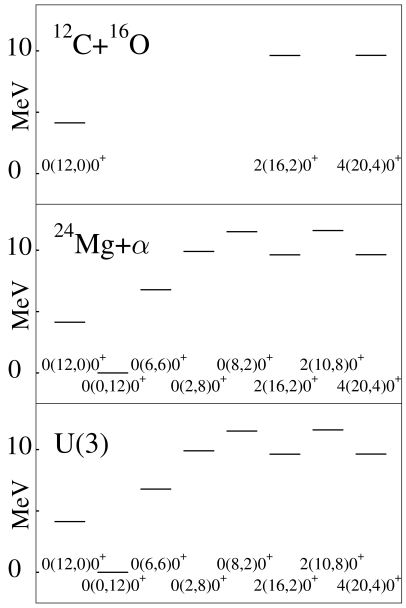

Figure 8. The spectra of the 0^+ states in the ^{28}Si nucleus and in its ^{24}Mg+^{4}He and ^{16}O+^{12}C clusterizations, as predicted by the Hamiltonian of MUSY. The states are characterized by the n$(\lambda,\mu)K^\pi$ quantum numbers, where n is the major shell excitation, and (λ,μ) refers to the SU(3) representation, i.e., the quadrupole deformation.

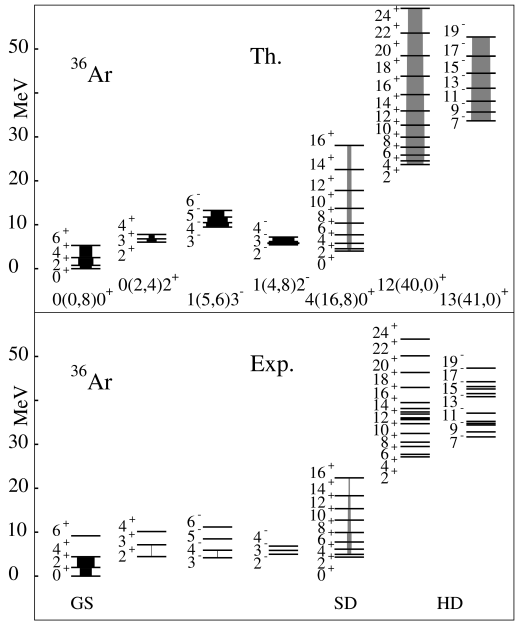

Figure 9. The spectrum of the MUSY in comparison with the experimental data of the ^{36}Ar nucleus. The real strength of the gray arrows (of the SD and HD bands) are 20 times of the illustrated ones.

Table 2. The parameters of the Hamiltonian and the E2 transitions obtained from a fitting procedure, and the $\hbar\omega$ values from the systematics.

	$\hbar\omega$	a	b	d	α^2
^{28}Si	12.10800	−0.13089	0.00043	1.07359	0.366
^{36}Ar	11.33540	−0.11060	0.00047	1.29467	0.466

3.4. Spontaneous Breaking and Cluster-Shell Duality

The nuclear deformation is a well-known example of spontaneous symmetry breaking: a deformed shape is obtained from the structure models of rotationally symmetric interactions. In other words, the Hamiltonian shows an O(3) symmetry, while the ground state (and many other states) of the system is deformed. The Elliott model illustrates this phenomenon in a very transparent way [5], though historically, this kind of studies were performed earlier in other theoretical frameworks [8–11].

As mentioned beforehand, the Hamiltonian of the Elliott model splits up into an intrinsic part (of the fast degrees of freedom) and a collective part (of the slow degrees of freedom). Both of them are rotationally symmetric, but the ground state of the intrinsic Hamiltonian is usually deformed, i.e., its SU(3) symmetry is (0,0), only exceptionally (corresponding to a spherical shape); more frequently, it indicates finite quadrupole deformation.

When a basic state of a definite SU(3) symmetry is present in the shell model space with a single multiplicity, then it is identical with the cluster configurations of the same symmetry: only one term is present in their shell-model expansion. In other words, the antisymmetrization can wash out the seemingly drastic difference between different configurations. It is known for a long time for some states in the ground region [3,4], and a similar situation is found for the shape isomers in the large-space calculations. Figures 10 and 11 show some clusterization of the ^{28}Si and ^{36}Ar nuclei, which show 100% overlap with each other and with the shell configurations.

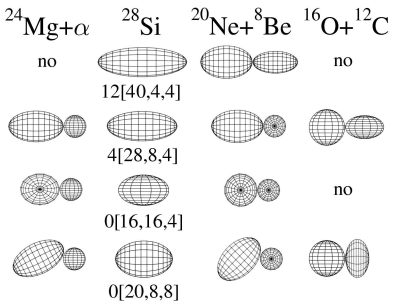

Figure 10. Shape of some states in ^{28}Si in increasing energy order. In [] parenthesis, the U(3) labels are indicated, while the first integer shows the major shell excitation quanta.

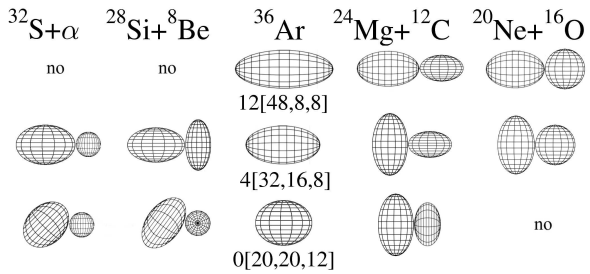

Figure 11. The same as Figure 10 for ^{36}Ar. Due to the antisymmetrization, the different cluster configurations are identical to each other as well as with the shell model state.

4. Summary and Conclusions

The multiconfigurational dynamical symmetry is the common intersection of the shell, collective, and cluster models for the multi-major-shell problem. Its algebraic structure, characterized by the group chain (2), shows that it is a straightforward extension of the U(3)-connection (chain (1)) between these fundamental structure models, found in 1958 for a single shell problem. MUSY is a composite symmetry in the sense that each configuration has a usual symmetry of chain (2), and in addition, it incorporates another symmetry that connects the configurations to each other. This connecting symmetry is an invariance with respect to transformations that act in the pseudo space of particle indices.

Due to its connecting role, MUSY can unify the description of various phenomena in atomic nuclei, like quadrupole deformation, shell structure, clusterization, and relations to reaction channels. Here we have shown how the shape isomers of a nucleus can be obtained from the study of the stability and self-consistency of the connecting U(3) symmetry (SCS method). Thus, it offers an alternative method to the well-known energy-surface calculations. It is remarkable that the stable U(3) symmetry is obtained from Nilsson model calculations with symmetry-breaking interactions; therefore, it is an emergent symmetry. Based on the U(3) symmetry, a selection rule can be applied for the allowed clusterizations, which define the possible reaction channels to populate the shape isomers (as well as for their decay).

For the spectrum calculations, MUSY has been applied so far with a very simple, dynamically symmetric Hamiltonian. It includes the following terms: a harmonic oscillator, the quadrupole-quadrupole interaction, and a cubic term; the latter distinguishes between prolate and oblate deformations. Nevertheless, this energy function can account for the gross features of the energy spectrum of different configurations in a large range of excitation energy and deformation. Due to the simplicity of the dynamically symmetric Hamiltonian MUSY can not compete with detailed (and more complicated) model calculations (e.g., shell model calculation) in the ground-state region. It is able, however, to describe the gross features of spectra of a great variety, which are usually treated in terms of different models.

We have shown here the application of MUSY to the ^{28}Si and ^{36}Ar nuclei. In order to illustrate its performance, we summarize here the conclusions of these applications.

For ^{28}Si, our SCS method gave several shape isomers, up to the linear alpha-chain configurations [46]. Special attention was focused from the experimental side on the prolate superdeformed state [47]. By reanalyzing the available data from (α, γ) and (p, γ) reactions, and extending them with new Gammasphere results from the ^{12}C(^{20}Ne,α)^{28}Si reaction, a candidate for the superdeformed state was obtained in complete agreement with our prediction on the moment of inertia, and on the favored reaction channels of ^{24}Mg+α and ^{12}C+^{16}O.

In the calculation of the energy spectrum, we have fitted the 3 parameters of our Hamiltonian to the low-lying well-established bands of the nucleus, describing them by the semimicroscopic algebraic quartet model. The high-lying core+α and ^{12}C+^{16}O cluster spectra (in full detail) could be obtained as a pure prediction without any parameter. Both of them show very good agreement with the experimental observation [44,46]. This study also answers a long-standing open question: the spectrum of the fine resolution ^{12}C+^{16}O resonances is that of the second, i.e., superdeformed valley.

In the case of the ^{36}Ar nucleus, the SD state was experimentally known before our study. The SCS method reproduced it with reasonable agreement [48], and it gave a prediction for the hyperdeformed (HD) state as well. The experimental study of the ^{12}C+^{24}Mg and ^{16}O+^{20}Ne reactions [49] revealed a sequence of resonances, which seem to correspond to the HD state with the predicted moment of inertia. It serves as a good candidate for the HD state. Multiple gamma-coincidence investigations of these states would be very interesting to check this conjecture.

The energy spectrum of the ^{36}Ar nucleus could also be described with the simple dynamically symmetric Hamiltonian in a unified manner, again for the low-lying shell-like states, the core+α configuration and the exotic clusterization. The deformation extends up to the HD state. In this case, the high-lying states were also taken into account in the fitting procedure, although with a very small weight (of 0.01, as compared to the 1.0 of the low-lying states). The reason, why extrapolation was not possible, like in the case of the ^{28}Si might be related to the fact that the low-lying spectrum is much less known.

In the case of ^{28}Si nucleus, MUSY described the spectra of the first and second (i.e., ground and superdeformed) valley in a unified way, while in the case of ^{36}Ar, it also included the hyperdeformed (third) minimum. It is an interesting question if it could also account for other, even more, exotic shape isomers.

Author Contributions: J.C.: conceptualization, methodology, writing; G.R.: investigation, software, visualization, J.D.: methodology, investigation, data curation. All authors have read and agreed to the published version of the manuscript.

Funding: This work was supported by the National Research, Development, and Innovation Fund of Hungary, financed under the K18 funding scheme with the project number K 128729.

Data Availability Statement: Data is contained within the article.

Conflicts of Interest: The authors declare no conflict of interest.

References

1. Elliott, J.P. Collective Motion in the Nuclear Shell Model. I. Classification Schemes for States of Mixed Configurations. *Proc. R. Soc. A* **1958**, *245*, 128–145.
2. Elliott, J.P. Collective Motion in the Nuclear Shell Model. II. The Introduction of Intrinsic Wave-Functions. *Proc. R. Soc. A* **1958**, *245*, 562–581.
3. Wildermuth, K.; Kanellopoulos, T. The "cluster model" of the atomic nuclei. *Nucl. Phys.* **1958**, *7*, 150–162. [CrossRef]
4. Bayman, B.F.; Bohr, A. On the connection between the cluster model and the SU3 coupling scheme for particles in a harmonic oscillator potential. *Nucl. Phys.* **1958**, *9*, 596–599. [CrossRef]
5. Cseh, J. Spontantaneous symmetry-breaking in Elliott-type models and the nuclear deformation. *Phys. Lett. B* **2019**, *793*, 59–64. [CrossRef]
6. Draayer, J.P. *Algebraic Approaches to Nuclear Structure*; Casten Harwood, R.F., Ed.; Academic: New York, NY, USA, 1993; p. 423.
7. Rowe, D.J. Microscopic theory of the nuclear collective model. *Rep. Prog. Phys.* **1985**, *48*, 1419–1480. [CrossRef]
8. Iachello, F.; Arima, A. *The Interacting Boson Model*; Cambridge University Press: Cambridge, UK, 1987; ISBN 9780521302821.
9. Reinhard, P.G.; Otten, E.W. Transition to deformed shapes as a nuclear Jahn-Teller effect. *Nucl. Phys. A* **1984**, *420*, 173–192. [CrossRef]
10. Nazarewicz, W. Nuclear deformations as a spontaneous symmetry breaking. *Int. J. Mod. Phys. E* **1993**, *2*, 51–69. [CrossRef]
11. Kirson, M.V.; Leviatan, A. Resolution of any interacting-boson-model Hamiltonian into intrinsic and collective parts. *Phys. Rev. Lett.* **1985**, *55*, 2846–2849. [CrossRef]
12. Cseh, J. Dual breaking of symmetries in algebraic models. *Eur. Phys. J. Spec. Top.* **2020**, *229*, 2543–2554. [CrossRef]
13. Cseh, J.; Lévai, G.; Algora ,A.; Hess, P.O.; Intasorn, A.; Kato, K. On the shell model connection of the cluster model. *Acta Phys. Hung.* **2000**, *12*, 119–122.
14. Rosensteel, G.; Rowe, D.J. Nuclear Sp(3, R). *Phys. Rev. Lett.* **1980**, *38*, 10–14. [CrossRef]
15. Rowe, D.J. The fundamental role of symmetry in nuclear models. *AIP Conf. Proc.* **2013**, *1541*, 104–136.
16. Launey, K.D.; Dytrych, T.; Sargsyan, G.H.; Baker, R.B.; Draayer, J. P. Emergent symplectic symmetry in atomic nuclei. *Eur. Phys. J. Spec. Top.* **2020**, *229*, 2429–2441. [CrossRef]
17. Tobin, G.K.; Ferriss, M.C.; Launey, K.D.; Dytrych, T.; Draayer, J.P.; Dreyfuss, A.C.; Bahri, C. Symplectic no-core shell-model approach to intermediate-mass nuclei. *Phys. Rev. C* **2014**, *89*, 034312. [CrossRef]
18. Dytrych, T.; Sviratcheva, K.D.; Draayer, J.P.; Bahri, C.; Vary, J.P. Ab initio symplectic no-core shell model. *J. Phys. G* **2008**, *35*, 123101. [CrossRef]
19. Dytrych, T.; Maris, P.; Launey, K.D.; Draayer, J.P.; Vary, J.P.; Langr, D.; Saule, E.; Caprio, M.A.; Catalyurek, U.; Sosonkina, M. Efficacy of the SU(3) scheme for ab initio large-scale calculations beyond the lightest nuclei. *Comp. Phys. Com.* **2016**, *207*, 202–210. [CrossRef]
20. Cseh, J. Algebraic models for shell-like quarteting of nucleons. *Phys. Lett. B* **2015**, *743*, 213–217. [CrossRef]
21. Rowe, D.J.; Rosensteel, G. Rotational bands in the u(3)-boson model. *Phys. Rev. C* **1982**, *25*, 3236–3238. [CrossRef]
22. Castanos, O.; Draayer, J.P. Contracted symplectic model with ds-shell applications. *Nucl. Phys. A* **1989**, *491*, 349–372. [CrossRef]
23. Cseh, J. Semimicroscopic algebraic description of nuclear cluster states. Vibron model coupled to the SU(3) shell model. *Phys. Lett. B* **1992**, *281*, 173–177. [CrossRef]
24. Cseh, J.; Lévai, G. Semimicroscopic Algebraic Cluster Model of Light Nuclei. I. Two-Cluster-Systems with Spin-Isospin-Free Interactions. *Ann. Phys.* **1994**, *230*, 165–200. [CrossRef]
25. Iachello, F. Algebraic approach to nuclear quasimolecular spectra. *Phys. Rev.* **1981**, *23*, 2778–2780. [CrossRef]
26. Iachello, F.; Levine, R.D. Algebraic approach to molecular rotation-vibration spectra. I. Diatomic molecules. *J. Chem. Phys.* **1982**, *77*, 3046–3055. [CrossRef]
27. Cseh, J. Microscopic structure and mathematical background of the multiconfigurational dynamical symmetry. *Phys. Rev. C* **2021**, *103*, 064322. [CrossRef]
28. Cseh, J. Multichannel dynamical symmetry and heavy ion resonances. *Phys. Rev. C* **1994**, *50*, 2240–2243. [CrossRef]
29. Cseh, J.; Kato, K. Multichannel dynamical symmetry and cluster-coexistence. *Phys. Rev. C* **2013**, *87*, 067301. [CrossRef]
30. Cseh, J. On the relation of the shell, collective and cluster models. *J. Phys. Conf. Ser.* **2015**, *580*, 012046. [CrossRef]
31. Cseh, J.; Riczu, G. Quartet excitations and cluster spectra in light nuclei. *Phys. Lett. B* **2016**, *757*, 312–316. [CrossRef]

32. Kramer, P.; Moshinsky, M. Group Theory of Harmonic Oscillators and Nuclear Structure. In *Group Theory and Its Applications*; Loebl, E.M., Ed.; Academic Press: New York, NY, USA, 1968; pp. 339–468. ISBN 978-1-4832-3188-4.
33. Rowe, D.J. Embedded Representations and Quasi-Dynamical Symmetry. In Proceedings of the Symposium in Honor of Jerry P Draayer's 60th Birthday, Playa del Carmen, Mexico, 18–21 February 2003.
34. Rochford, P.; Rowe, D.J. The survival of rotor and SU(3) bands under strong spin-orbit symmetry mixing. *Phys. Lett. B* **1988**, *210*, 5–9. [CrossRef]
35. Rochford, P.; Rowe, D.J.; Repka, J. Dynamic structure and embedded representation in physics: The group theory of the adiabatic approximation. *J. Math. Phys.* **1988**, *29*, 572–577.
36. Cseh, J.; Riczu, G.; Darai, J. Shape isomers of light nuclei from the stability and consistency of the SU(3) symmetry. *Phys. Lett. B* **2009**, *795*, 160–164. [CrossRef]
37. Jarrio, M.; Wood, J.L.; Rowe, D.J. The SU(3) structure of rotational states in heavy deformed nuclei. *Nucl. Phys. A* **1991**, *528*, 409–435. [CrossRef]
38. Hess, P.O.; Algora, A.; Hunyadi, M.; Cseh, J. Configuration-mixed effective SU(3) symmetries. *Eur. Phys. J. A* **2002**, *15*, 449–454. [CrossRef]
39. Leander, G.; Larsson, S.E. Potential-energy surfaces for the doubly even N=Z nuclei. *Nucl. Phys. A* **1975**, *239*, 93–113. [CrossRef]
40. Merchant, A.C.; Rae, W.D.M. Systematics of alpha-chain states in 4N-nuclei. *Nucl. Phys. A* **1992**, *549*, 431–438. [CrossRef]
41. Zhang, J.; Rae, W.D.M. Systematics of 2-dimensional α-cluster configurations in 4N nuclei from ^{12}C to ^{44}Ti. *Nucl. Phys. A* **1993**, *564*, 252–270. [CrossRef]
42. Zhang, J.; Rae, W.D.M.; Merchant, A.C. Systematics of some 3-dimensional α-cluster configurations in 4N nuclei from ^{16}O to ^{44}Ti. *Nucl. Phys. A* **1994**, *575*, 61–71. [CrossRef]
43. Blomqvist, J.; Molinari, A. Collective 0^- vibrations in even spherical nuclei with tensor forces. *Nucl. Phys. A* **1968**, *106*, 545–569. [CrossRef]
44. Adsley, P.; Jenkins, D.G.; Cseh, J.; Dimitriova, S.S.; Brummer, J.W.; Li, K.C.W.; Marín-Lámbarri, D.J.; Lukyanov, K.; Kheswa, N.Y.; Neveling, R.; et al. Alpha clustering in ^{28}Si probed through the identification of high-lying 0^+ states. *Phys. Rev. C* **2017**, *95*, 024319. [CrossRef]
45. Akiyama, Y.; Draayer, J.P. A User's guide to Fortran programs for Wigner and Racah coefficients of SU3. *Comp. Phys. Com.* **1973**, *5*, 405–415. [CrossRef]
46. Darai, J.; Cseh, J.; Jenkins, D.G.; Cseh, J. Shape isomers and clusterization in the ^{28}Si nucleus. *Phys. Rev. C.* **2012**, *86*, 064309. [CrossRef]
47. Jenkins, D.G.; Lister, C.J.; Carpenter, M.P.; Chowdury, P.; Hammond, N.J.; Janssens, R.V.F.; Khoo, T.L.; Lauritsen, T.; Seweryniak, D.; Davinson, T.; et al. Candidate superdeformed band in ^{28}Si. *Phys. Rev. C* **2012**, *86*, 064308. [CrossRef]
48. Cseh, J.; Darai, J.; Sciani, W.; Otani, Y.; Lepine-Szily, A.; Benjamim, E.A.; Chamon, L.C.; Lichtenthaler Filho, R. Elongated shape isomers in the ^{36}Ar nucleus. *Phys. Rev. C* **2009**, *80*, 034320. [CrossRef]
49. Sciani, W.; Otani, Y.; Lepine-Szily, A.; Benjamim, E.A.; Chamon, L.C.; Lichtenthaler Filho, R.; Cseh, J.; Darai, J. Possible hyperdeformed band in ^{36}Ar observed in ^{12}C+^{24}Mg elastic scattering. *Phys. Rev. C* **2009**, *80*, 034319. [CrossRef]